

A Search for $Wb\bar{b}$ and WH Production in $p\bar{p}$ Collisions at $\sqrt{s} = 1.96$ TeV

V.M. Abazov,³³ B. Abbott,⁷⁰ M. Abolins,⁶¹ B.S. Acharya,²⁷ M. Adams,⁴⁸ T. Adams,⁴⁶ M. Agelou,¹⁷ J.-L. Agram,¹⁸ S.H. Ahn,²⁹ M. Ahsan,⁵⁵ G.D. Alexeev,³³ G. Alkhazov,³⁷ A. Alton,⁶⁰ G. Alverson,⁵⁹ G.A. Alves,² M. Anastasoiae,³² S. Anderson,⁴² B. Andrieu,¹⁶ Y. Arnoud,¹³ A. Askew,⁷⁴ B. Åsman,³⁸ O. Atramentov,⁵³ C. Autermann,²⁰ C. Avila,⁷ F. Badaud,¹² A. Baden,⁵⁷ B. Baldin,⁴⁷ P.W. Balm,³¹ S. Banerjee,²⁷ E. Barberis,⁵⁹ P. Bargassa,⁷⁴ P. Baringer,⁵⁴ C. Barnes,⁴⁰ J. Barreto,² J.F. Bartlett,⁴⁷ U. Bassler,¹⁶ D. Bauer,⁵¹ A. Bean,⁵⁴ S. Beauceron,¹⁶ M. Begel,⁶⁶ A. Bellavance,⁶³ S.B. Beri,²⁶ G. Bernardi,¹⁶ R. Bernhard,^{47,*} I. Bertram,³⁹ M. Besançon,¹⁷ R. Beuselinck,⁴⁰ V.A. Bezzubov,³⁶ P.C. Bhat,⁴⁷ V. Bhatnagar,²⁶ M. Binder,²⁴ K.M. Black,⁵⁸ I. Blackler,⁴⁰ G. Blazey,⁴⁹ F. Blekman,³¹ S. Blessing,⁴⁶ D. Bloch,¹⁸ U. Blumenschein,²² A. Boehnlein,⁴⁷ O. Boeriu,⁵² T.A. Bolton,⁵⁵ F. Borcherding,⁴⁷ G. Borissov,³⁹ K. Bos,³¹ T. Bose,⁶⁵ A. Brandt,⁷² R. Brock,⁶¹ G. Brooijmans,⁶⁵ A. Bross,⁴⁷ N.J. Buchanan,⁴⁶ D. Buchholz,⁵⁰ M. Buehler,⁴⁸ V. Buescher,²² S. Burdin,⁴⁷ T.H. Burnett,⁷⁶ E. Busato,¹⁶ J.M. Butler,⁵⁸ J. Bystricky,¹⁷ W. Carvalho,³ B.C.K. Casey,⁷¹ N.M. Cason,⁵² H. Castilla-Valdez,³⁰ S. Chakrabarti,²⁷ D. Chakraborty,⁴⁹ K.M. Chan,⁶⁶ A. Chandra,²⁷ D. Chapin,⁷¹ F. Charles,¹⁸ E. Cheu,⁴² L. Chevalier,¹⁷ D.K. Cho,⁶⁶ S. Choi,⁴⁵ T. Christiansen,²⁴ L. Christofek,⁵⁴ D. Claes,⁶³ B. Clément,¹⁸ C. Clément,³⁸ Y. Coadou,⁵ M. Cooke,⁷⁴ W.E. Cooper,⁴⁷ D. Coppage,⁵⁴ M. Corcoran,⁷⁴ J. Coss,¹⁹ A. Cothenet,¹⁴ M.-C. Cousinou,¹⁴ S. Crépé-Renaudin,¹³ M. Cristetiu,⁴⁵ M.A.C. Cummings,⁴⁹ D. Cutts,⁷¹ H. da Motta,² B. Davies,³⁹ G. Davies,⁴⁰ G.A. Davis,⁵⁰ K. De,⁷² P. de Jong,³¹ S.J. de Jong,³² E. De La Cruz-Burelo,³⁰ C. De Oliveira Martins,³ S. Dean,⁴¹ F. Déliot,¹⁷ P.A. Delsart,¹⁹ M. Demarteau,⁴⁷ R. Demina,⁶⁶ P. Demine,¹⁷ D. Denisov,⁴⁷ S.P. Denisov,³⁶ S. Desai,⁶⁷ H.T. Diehl,⁴⁷ M. Diesburg,⁴⁷ M. Doidge,³⁹ H. Dong,⁶⁷ S. Doulas,⁵⁹ L. Duflot,¹⁵ S.R. Dugad,²⁷ A. Duperrin,¹⁴ J. Dyer,⁶¹ A. Dyshkant,⁴⁹ M. Eads,⁴⁹ D. Edmunds,⁶¹ T. Edwards,⁴¹ J. Ellison,⁴⁵ J. Elmsheuser,²⁴ J.T. Eltzroth,⁷² V.D. Elvira,⁴⁷ S. Eno,⁵⁷ P. Ermolov,³⁵ O.V. Eroshin,³⁶ J. Estrada,⁴⁷ D. Evans,⁴⁰ H. Evans,⁶⁵ A. Evdokimov,³⁴ V.N. Evdokimov,³⁶ J. Fast,⁴⁷ S.N. Fataki,⁵⁸ L. Feligioni,⁵⁸ T. Ferbel,⁶⁶ F. Fiedler,²⁴ F. Filthaut,³² W. Fisher,⁶⁴ H.E. Fisk,⁴⁷ M. Fortner,⁴⁹ H. Fox,²² W. Freeman,⁴⁷ S. Fu,⁴⁷ S. Fuess,⁴⁷ T. Gadfort,⁷⁶ C.F. Galea,³² E. Gallas,⁴⁷ E. Galyaev,⁵² C. Garcia,⁶⁶ A. Garcia-Bellido,⁷⁶ J. Gardner,⁵⁴ V. Gavrilov,³⁴ P. Gay,¹² D. Gelé,¹⁸ R. Gelhaus,⁴⁵ K. Genser,⁴⁷ C.E. Gerber,⁴⁸ Y. Gershtein,⁷¹ G. Ginther,⁶⁶ T. Golling,²¹ B. Gómez,⁷ K. Gounder,⁴⁷ A. Goussiou,⁵² P.D. Grannis,⁶⁷ S. Greder,¹⁸ H. Greenlee,⁴⁷ Z.D. Greenwood,⁵⁶ E.M. Gregores,⁴ Ph. Gris,¹² J.-F. Grivaz,¹⁵ L. Groer,⁶⁵ S. Grünendahl,⁴⁷ M.W. Grünewald,²⁸ S.N. Gurzhev,³⁶ G. Gutierrez,⁴⁷ P. Gutierrez,⁷⁰ A. Haas,⁶⁵ N.J. Hadley,⁵⁷ S. Hagopian,⁴⁶ I. Hall,⁷⁰ R.E. Hall,⁴⁴ C. Han,⁶⁰ L. Han,⁴¹ K. Hanagaki,⁴⁷ K. Harder,⁵⁵ R. Harrington,⁵⁹ J.M. Hauptman,⁵³ R. Hauser,⁶¹ J. Hays,⁵⁰ T. Hebbeker,²⁰ D. Hedin,⁴⁹ J.M. Heinmiller,⁴⁸ A.P. Heinson,⁴⁵ U. Heintz,⁵⁸ C. Hensel,⁵⁴ G. Hesketh,⁵⁹ M.D. Hildreth,⁵² R. Hirosky,⁷⁵ J.D. Hobbs,⁶⁷ B. Hoeneisen,¹¹ M. Hohlfeld,²³ S.J. Hong,²⁹ R. Hooper,⁷¹ P. Houben,³¹ Y. Hu,⁶⁷ J. Huang,⁵¹ I. Iashvili,⁴⁵ R. Illingworth,⁴⁷ A.S. Ito,⁴⁷ S. Jabeen,⁵⁴ M. Jaffré,¹⁵ S. Jain,⁷⁰ V. Jain,⁶⁸ K. Jakobs,²² A. Jenkins,⁴⁰ R. Jesik,⁴⁰ K. Johns,⁴² M. Johnson,⁴⁷ A. Jonckheere,⁴⁷ P. Jonsson,⁴⁰ H. Jöstlein,⁴⁷ A. Juste,⁴⁷ M.M. Kado,⁴³ D. Käfer,²⁰ W. Kahl,⁵⁵ S. Kahn,⁶⁸ E. Kajfasz,¹⁴ A.M. Kalinin,³³ J. Kalk,⁶¹ D. Karmanov,³⁵ J. Kasper,⁵⁸ D. Kau,⁴⁶ R. Kehoe,⁷³ S. Kermiche,¹⁴ S. Kesisoglou,⁷¹ A. Khanov,⁶⁶ A. Kharchilava,⁵² Y.M. Kharzheev,³³ K.H. Kim,²⁹ B. Klima,⁴⁷ M. Klute,²¹ J.M. Kohli,²⁶ M. Kopal,⁷⁰ V.M. Korablev,³⁶ J. Kotcher,⁶⁸ B. Kothari,⁶⁵ A. Koubarovsky,³⁵ A.V. Kozelov,³⁶ J. Kozminski,⁶¹ S. Krzywdzinski,⁴⁷ S. Kuleshov,³⁴ Y. Kulik,⁴⁷ S. Kunori,⁵⁷ A. Kupco,¹⁷ T. Kurča,¹⁹ S. Lager,³⁸ N. Lahrichi,¹⁷ G. Landsberg,⁷¹ J. Lazoflores,⁴⁶ A.-C. Le Bihan,¹⁸ P. Lebrun,¹⁹ S.W. Lee,²⁹ W.M. Lee,⁴⁶ A. Leflat,³⁵ F. Lehner,^{47,*} C. Leonidopoulos,⁶⁵ P. Lewis,⁴⁰ J. Li,⁷² Q.Z. Li,⁴⁷ J.G.R. Lima,⁴⁹ D. Lincoln,⁴⁷ S.L. Linn,⁴⁶ J. Linnemann,⁶¹ V.V. Lipaev,³⁶ R. Lipton,⁴⁷ L. Lobo,⁴⁰ A. Lobodenko,³⁷ M. Lokajicek,¹⁰ A. Lounis,¹⁸ H.J. Lubatti,⁷⁶ L. Lueking,⁴⁷ M. Lynker,⁵² A.L. Lyon,⁴⁷ A.K.A. Maciel,⁴⁹ R.J. Madaras,⁴³ P. Mättig,²⁵ A. Magerkurth,⁶⁰ A.-M. Magnan,¹³ N. Makovec,¹⁵ P.K. Mal,²⁷ S. Malik,⁵⁶ V.L. Malyshev,³³ H.S. Mao,⁶ Y. Maravin,⁴⁷ M. Martens,⁴⁷ S.E.K. Mattingly,⁷¹ A.A. Mayorov,³⁶ R. McCarthy,⁶⁷ R. McCroskey,⁴² D. Meder,²³ H.L. Melanson,⁴⁷ A. Melnitchouk,⁶² M. Merkin,³⁵ K.W. Merritt,⁴⁷ A. Meyer,²⁰ H. Miettinen,⁷⁴ D. Mihalcea,⁴⁹ J. Mitrevski,⁶⁵ N. Mokhov,⁴⁷ J. Molina,³ N.K. Mondal,²⁷ H.E. Montgomery,⁴⁷ R.W. Moore,⁵ G.S. Muanza,¹⁹ M. Mulders,⁴⁷ Y.D. Mutaf,⁶⁷ E. Nagy,¹⁴ M. Narain,⁵⁸ N.A. Naumann,³² H.A. Neal,⁶⁰ J.P. Negret,⁷ S. Nelson,⁴⁶ P. Neustroev,³⁷ C. Noeding,²² A. Nomerotski,⁴⁷ S.F. Novaes,⁴ T. Nunnemann,²⁴ E. Nurse,⁴¹ V. O'Dell,⁴⁷ D.C. O'Neil,⁵ V. Oguri,³ N. Oliveira,³ N. Oshima,⁴⁷ G.J. Otero y Garzón,⁴⁸ P. Padley,⁷⁴ N. Parashar,⁵⁶ J. Park,²⁹ S.K. Park,²⁹ J. Parsons,⁶⁵ R. Partridge,⁷¹ N. Parua,⁶⁷ A. Patwa,⁶⁸ P.M. Perea,⁴⁵ E. Perez,¹⁷ O. Peters,³¹

P. Pétroff,¹⁵ M. Petteni,⁴⁰ L. Phaf,³¹ R. Piegaia,¹ P.L.M. Podesta-Lerma,³⁰ V.M. Podstavkov,⁴⁷ Y. Pogorelov,⁵² B.G. Pope,⁶¹ W.L. Prado da Silva,³ H.B. Prosper,⁴⁶ S. Protopopescu,⁶⁸ M.B. Przybycien,^{50,†} J. Qian,⁶⁰ A. Quadt,²¹ B. Quinn,⁶² K.J. Rani,²⁷ P.A. Rapidis,⁴⁷ P.N. Ratoff,³⁹ N.W. Reay,⁵⁵ S. Reucroft,⁵⁹ M. Rijssenbeek,⁶⁷ I. Ripp-Baudot,¹⁸ F. Rizatdinova,⁵⁵ C. Royon,¹⁷ P. Rubinov,⁴⁷ R. Ruchti,⁵² G. Sajot,¹³ A. Sánchez-Hernández,³⁰ M.P. Sanders,⁴¹ A. Santoro,³ G. Savage,⁴⁷ L. Sawyer,⁵⁶ T. Scanlon,⁴⁰ R.D. Schamberger,⁶⁷ H. Schellman,⁵⁰ P. Schieferdecker,²⁴ C. Schmitt,²⁵ A.A. Schukin,³⁶ A. Schwartzman,⁶⁴ R. Schwienhorst,⁶¹ S. Sengupta,⁴⁶ H. Severini,⁷⁰ E. Shabalina,⁴⁸ M. Shamim,⁵⁵ V. Shary,¹⁷ W.D. Shephard,⁵² D. Shpakov,⁵⁹ R.A. Sidwell,⁵⁵ V. Simak,⁹ V. Sirotenko,⁴⁷ P. Skubic,⁷⁰ P. Slattery,⁶⁶ R.P. Smith,⁴⁷ K. Smolek,⁹ G.R. Snow,⁶³ J. Snow,⁶⁹ S. Snyder,⁶⁸ S. Söldner-Rembold,⁴¹ X. Song,⁴⁹ Y. Song,⁷² L. Sonnenschein,⁵⁸ A. Sopczak,³⁹ M. Sosebee,⁷² K. Soustruznik,⁸ M. Souza,² B. Spurlock,⁷² N.R. Stanton,⁵⁵ J. Stark,¹³ J. Steele,⁵⁶ G. Steinbrück,⁶⁵ K. Stevenson,⁵¹ V. Stolin,³⁴ A. Stone,⁴⁸ D.A. Stoyanova,³⁶ J. Strandberg,³⁸ M.A. Strang,⁷² M. Strauss,⁷⁰ R. Ströhmer,²⁴ M. Strovink,⁴³ L. Stutte,⁴⁷ S. Sumowidagdo,⁴⁶ A. Sznajder,³ M. Talby,¹⁴ P. Tamburello,⁴² W. Taylor,⁵ P. Telford,⁴¹ J. Temple,⁴² S. Tentindo-Repond,⁴⁶ E. Thomas,¹⁴ B. Thooris,¹⁷ M. Tomoto,⁴⁷ T. Toole,⁵⁷ J. Torborg,⁵² S. Towers,⁶⁷ T. Trefzger,²³ S. Trincaz-Duvold,¹⁶ B. Tuchming,¹⁷ C. Tully,⁶⁴ A.S. Turcot,⁶⁸ P.M. Tuts,⁶⁵ L. Uvarov,³⁷ S. Uvarov,³⁷ S. Uzunyan,⁴⁹ B. Vachon,⁵ R. Van Kooten,⁵¹ W.M. van Leeuwen,³¹ N. Varelas,⁴⁸ E.W. Varnes,⁴² I.A. Vasilyev,³⁶ M. Vaupel,²⁵ P. Verdier,¹⁵ L.S. Vertogradov,³³ M. Verzocchi,⁵⁷ F. Villeneuve-Seguier,⁴⁰ J.-R. Vlimant,¹⁶ E. Von Toerne,⁵⁵ M. Vreeswijk,³¹ T. Vu Anh,¹⁵ H.D. Wahl,⁴⁶ R. Walker,⁴⁰ L. Wang,⁵⁷ Z.-M. Wang,⁶⁷ J. Warchol,⁵² M. Warsinsky,²¹ G. Watts,⁷⁶ M. Wayne,⁵² M. Weber,⁴⁷ H. Weerts,⁶¹ M. Wegner,²⁰ N. Wermes,²¹ A. White,⁷² V. White,⁴⁷ D. Whiteson,⁴³ D. Wicke,⁴⁷ D.A. Wijngaarden,³² G.W. Wilson,⁵⁴ S.J. Wimpenny,⁴⁵ J. Wittlin,⁵⁸ M. Wobisch,⁴⁷ J. Womersley,⁴⁷ D.R. Wood,⁵⁹ T.R. Wyatt,⁴¹ Q. Xu,⁶⁰ N. Xuan,⁵² R. Yamada,⁴⁷ M. Yan,⁵⁷ T. Yasuda,⁴⁷ Y.A. Yatsunenko,³³ Y. Yen,²⁵ K. Yip,⁶⁸ S.W. Youn,⁵⁰ J. Yu,⁷² A. Yurkewicz,⁶¹ A. Zabi,¹⁵ A. Zatserklyaniy,⁴⁹ M. Zdrrazil,⁶⁷ C. Zeitnitz,²³ D. Zhang,⁴⁷ X. Zhang,⁷⁰ T. Zhao,⁷⁶ Z. Zhao,⁶⁰ B. Zhou,⁶⁰ J. Zhu,⁵⁷ M. Zielinski,⁶⁶ D. Ziemska,⁵¹ A. Ziemiński,⁵¹ R. Zitoun,⁶⁷ V. Zutshi,⁴⁹ E.G. Zverev,³⁵ and A. Zylberstejn¹⁷ (DØ Collaboration)

¹ Universidad de Buenos Aires, Buenos Aires, Argentina

² LAFEX, Centro Brasileiro de Pesquisas Físicas, Rio de Janeiro, Brazil

³ Universidade do Estado do Rio de Janeiro, Rio de Janeiro, Brazil

⁴ Instituto de Física Teórica, Universidade Estadual Paulista, São Paulo, Brazil

⁵ Simon Fraser University, Burnaby, Canada, University of Alberta, Edmonton, Canada, McGill University, Montreal, Canada and York University, Toronto, Canada

⁶ Institute of High Energy Physics, Beijing, People's Republic of China

⁷ Universidad de los Andes, Bogotá, Colombia

⁸ Charles University, Center for Particle Physics, Prague, Czech Republic

⁹ Czech Technical University, Prague, Czech Republic

¹⁰ Institute of Physics, Academy of Sciences, Center for Particle Physics, Prague, Czech Republic

¹¹ Universidad San Francisco de Quito, Quito, Ecuador

¹² Laboratoire de Physique Corpusculaire, IN2P3-CNRS, Université Blaise Pascal, Clermont-Ferrand, France

¹³ Laboratoire de Physique Subatomique et de Cosmologie, IN2P3-CNRS, Université de Grenoble 1, Grenoble, France

¹⁴ CPPM, IN2P3-CNRS, Université de la Méditerranée, Marseille, France

¹⁵ Laboratoire de l'Accélérateur Linéaire, IN2P3-CNRS, Orsay, France

¹⁶ LPNHE, Universités Paris VI and VII, IN2P3-CNRS, Paris, France

¹⁷ DAPNIA/Service de Physique des Particules, CEA, Saclay, France

¹⁸ IReS, IN2P3-CNRS, Université Louis Pasteur, Strasbourg, France and Université de Haute Alsace, Mulhouse, France

¹⁹ Institut de Physique Nucléaire de Lyon, IN2P3-CNRS, Université Claude Bernard, Villeurbanne, France

²⁰ RWTH Aachen, III. Physikalisches Institut A, Aachen, Germany

²¹ Universität Bonn, Physikalisches Institut, Bonn, Germany

²² Universität Freiburg, Physikalisches Institut, Freiburg, Germany

²³ Universität Mainz, Institut für Physik, Mainz, Germany

²⁴ Ludwig-Maximilians-Universität München, München, Germany

²⁵ Fachbereich Physik, University of Wuppertal, Wuppertal, Germany

²⁶ Panjab University, Chandigarh, India

²⁷ Tata Institute of Fundamental Research, Mumbai, India

²⁸ University College Dublin, Dublin, Ireland

²⁹ Korea Detector Laboratory, Korea University, Seoul, Korea

³⁰ CINVESTAV, Mexico City, Mexico

³¹ FOM-Institute NIKHEF and University of Amsterdam/NIKHEF, Amsterdam, The Netherlands

³² University of Nijmegen/NIKHEF, Nijmegen, The Netherlands

³³ Joint Institute for Nuclear Research, Dubna, Russia

³⁴*Institute for Theoretical and Experimental Physics, Moscow, Russia*
³⁵*Moscow State University, Moscow, Russia*
³⁶*Institute for High Energy Physics, Protvino, Russia*
³⁷*Petersburg Nuclear Physics Institute, St. Petersburg, Russia*
³⁸*Lund University, Lund, Sweden, Royal Institute of Technology and Stockholm University, Stockholm, Sweden and Uppsala University, Uppsala, Sweden*
³⁹*Lancaster University, Lancaster, United Kingdom*
⁴⁰*Imperial College, London, United Kingdom*
⁴¹*University of Manchester, Manchester, United Kingdom*
⁴²*University of Arizona, Tucson, Arizona 85721, USA*
⁴³*Lawrence Berkeley National Laboratory and University of California, Berkeley, California 94720, USA*
⁴⁴*California State University, Fresno, California 93740, USA*
⁴⁵*University of California, Riverside, California 92521, USA*
⁴⁶*Florida State University, Tallahassee, Florida 32306, USA*
⁴⁷*Fermi National Accelerator Laboratory, Batavia, Illinois 60510, USA*
⁴⁸*University of Illinois at Chicago, Chicago, Illinois 60607, USA*
⁴⁹*Northern Illinois University, DeKalb, Illinois 60115, USA*
⁵⁰*Northwestern University, Evanston, Illinois 60208, USA*
⁵¹*Indiana University, Bloomington, Indiana 47405, USA*
⁵²*University of Notre Dame, Notre Dame, Indiana 46556, USA*
⁵³*Iowa State University, Ames, Iowa 50011, USA*
⁵⁴*University of Kansas, Lawrence, Kansas 66045, USA*
⁵⁵*Kansas State University, Manhattan, Kansas 66506, USA*
⁵⁶*Louisiana Tech University, Ruston, Louisiana 71272, USA*
⁵⁷*University of Maryland, College Park, Maryland 20742, USA*
⁵⁸*Boston University, Boston, Massachusetts 02215, USA*
⁵⁹*Northeastern University, Boston, Massachusetts 02115, USA*
⁶⁰*University of Michigan, Ann Arbor, Michigan 48109, USA*
⁶¹*Michigan State University, East Lansing, Michigan 48824, USA*
⁶²*University of Mississippi, University, Mississippi 38677, USA*
⁶³*University of Nebraska, Lincoln, Nebraska 68588, USA*
⁶⁴*Princeton University, Princeton, New Jersey 08544, USA*
⁶⁵*Columbia University, New York, New York 10027, USA*
⁶⁶*University of Rochester, Rochester, New York 14627, USA*
⁶⁷*State University of New York, Stony Brook, New York 11794, USA*
⁶⁸*Brookhaven National Laboratory, Upton, New York 11973, USA*
⁶⁹*Langston University, Langston, Oklahoma 73050, USA*
⁷⁰*University of Oklahoma, Norman, Oklahoma 73019, USA*
⁷¹*Brown University, Providence, Rhode Island 02912, USA*
⁷²*University of Texas, Arlington, Texas 76019, USA*
⁷³*Southern Methodist University, Dallas, Texas 75275, USA*
⁷⁴*Rice University, Houston, Texas 77005, USA*
⁷⁵*University of Virginia, Charlottesville, Virginia 22901, USA*
⁷⁶*University of Washington, Seattle, Washington 98195, USA*

(Dated: February 3, 2008)

We present a search for $Wb\bar{b}$ production in $p\bar{p}$ collisions at $\sqrt{s} = 1.96$ TeV in events containing one electron, an imbalance in transverse momentum, and two b -tagged jets. Using 174 pb^{-1} of integrated luminosity accumulated by the DØ experiment at the Fermilab Tevatron collider, and the standard-model description of such events, we set a 95% C.L. upper limit on $Wb\bar{b}$ production of 6.6 pb for b quarks with transverse momenta $p_T^b > 20$ GeV and $b\bar{b}$ separation in pseudorapidity–azimuth space $\Delta\mathcal{R}_{b\bar{b}} > 0.75$. Restricting the search to optimized $b\bar{b}$ mass intervals provides upper limits on WH production of 9.0–12.2 pb, for Higgs-boson masses of 105–135 GeV.

PACS numbers: 13.85Qk, 13.85.Rm

The Higgs boson is the only scalar elementary particle expected in the standard model (SM). Its discovery would be a major success for the SM and would provide further insights into the electroweak symmetry breaking mechanism. The constraints from precision measurements [1]

favor a Higgs boson sufficiently light to be accessible at the Fermilab Tevatron collider. Although the expected luminosity necessary for its discovery is higher than obtained thus far, the special role of the Higgs boson in the SM justifies extensive searches for a Higgs-like particle in-

dependent of expected sensitivity. Such studies also provide an opportunity to investigate the main backgrounds, and in particular the interesting and thus far unobserved $Wb\bar{b}$ production process.

In this Letter, we present a search for a Higgs (H) boson with mass m_H between 105 and 135 GeV, in the production channel $p\bar{p} \rightarrow WH \rightarrow e\nu b\bar{b}$, at $\sqrt{s} = 1.96$ TeV. The expected WH cross section is of the order of 0.2 pb for this mass range [2]. Our search is based on an integrated luminosity of 174 ± 11 pb $^{-1}$ accumulated by the DØ experiment during 2002 and 2003.

The experimental signature of $WH \rightarrow e\nu b\bar{b}$ relies on a final state with one high p_T electron, two b jets and large imbalance in transverse momentum (\cancel{E}_T) resulting from the undetected neutrino. The dominant backgrounds to WH production are from $Wb\bar{b}$, $t\bar{t}$ and single top-quark production. The signal to background ratio is improved by requiring exactly two jets in the final state, because the fraction of $t\bar{t}$ events that contain at most two reconstructed jets is small. We use the high statistics $W+2$ jets data to check the validity of our simulation, but restrict the selection to $W+2$ b jets for the final results.

The DØ detector includes a magnetic tracking system surrounded by a uranium/liquid-argon calorimeter, which is enclosed in a muon spectrometer. The tracking system consists of a silicon microstrip tracker (SMT) and a central fiber tracker (CFT), both located within a 2 T superconducting solenoidal magnet [3]. The SMT and CFT have designs optimized for tracking and vertexing capabilities for pseudorapidities $|\eta| < 3$ and $|\eta| < 2.5$, respectively [4]. The calorimeter has a central section (CC) covering η up to $|\eta| \approx 1.1$, and two end calorimeters (EC) extending coverage to $|\eta| \approx 4.2$, each housed in a separate cryostat [5]. For particle identification, the calorimeter is divided into an electromagnetic (EM) section, followed by fine (FH) and coarse (CH) hadronic sections. Scintillators between the CC and EC cryostats provide additional sampling of developing showers for $1.1 < |\eta| < 1.4$. The muon system consists of a layer of tracking detectors and scintillation trigger counters in front of 1.8 T toroids, followed by two similar layers behind the toroids, which provide muon tracking for $|\eta| < 2$. The luminosity is measured using scintillator arrays located in front of the EC cryostats, covering $2.7 < |\eta| < 4.4$.

Event selection starts with the requirement of an isolated electron, with $p_T > 20$ GeV, in the central region of $|\eta| < 1.1$, but away from boundaries of calorimeter modules at periodic azimuthal angle (φ) values [6]. Such electrons are required to trigger the event. The average trigger efficiency is $(94 \pm 3)\%$ for $W+2$ jets events. Electron candidates are selected by requiring: (i) at least 90% of the energy in a cone of radius $\Delta\mathcal{R} = \sqrt{(\Delta\varphi)^2 + (\Delta\eta)^2} = 0.2$, relative to the shower axis, is deposited in the EM layers of the calorimeter, i.e., EM fraction $emf > 0.9$; (ii) isolation, i.e., that the total energy in a cone of $\Delta\mathcal{R} < 0.4$ centered on the same axis does not exceed the recon-

structed electron energy by more than 10%; (iii) that the energy cluster of the electron candidate has the characteristics of an EM shower, as determined by the standard DØ shower-shape criteria [6]; (iv) that there is a track pointing to the EM cluster. These four criteria define the initial electron candidates. Electron selection is further refined using an electron likelihood discriminant based on the above estimators, as well as on additional tracking information. The combined reconstruction and identification efficiency is determined from a $Z \rightarrow e^+e^-$ sample to be $(74 \pm 4)\%$ per electron.

To select W bosons, we require $\cancel{E}_T > 25$ GeV. Events with a second isolated lepton (e or μ [7]) with $p_T > 15$ GeV and $|\eta| < 2.4$ are rejected to suppress $Z +$ jets and $t\bar{t}$ backgrounds. Only events with a primary vertex at $|z| < 60$ cm relative to the center of the detector are retained. At least two jets with $p_T > 20$ GeV and $|\eta| < 2.5$ are then required. A jet is defined as a cluster of calorimeter towers within a radius $\Delta\mathcal{R} = 0.5$ [8], having: (i) $0.05 < emf < 0.95$; (ii) less than 40% of its energy in the CH section of the calorimeter; (iii) a distance $\Delta\mathcal{R}$ to any initial electron candidate greater than 0.5. The average jet reconstruction and identification efficiency is $(95 \pm 5)\%$, as determined from $\gamma +$ jet events. For selecting b jets, we use an impact-parameter based algorithm [9], which has been cross-checked with a secondary-vertex reconstruction algorithm.

To improve calorimeter performance, before reconstructing the calorimeter objects, we use an algorithm that suppresses cells with negative energy (originating from fluctuations in noise) and cells with energies four standard deviations below the average electronics noise (σ_n), when they do not neighbor a cell of higher energy, $E > 4\sigma_n$. The EM scale is calibrated using the peak in the $Z \rightarrow e^+e^-$ reconstructed mass, and jet energies are then corrected to the EM scale using $\gamma +$ jet events. These energy corrections, and the transverse momenta of any muons in the event, are propagated into the calculation of the \cancel{E}_T , which is estimated initially using all (unsuppressed) calorimeter cells.

The DØ detector simulation based on GEANT [10] and the reconstruction and analysis chain used for data are also used for obtaining expectations from the standard model, which are normalized to cross sections measured in data, or to calculations when no such measurements are available. Small additional energy smearing in \cancel{E}_T and in the energy of the simulated electrons is used to obtain better agreement between data and simulation.

Before applying b tagging, we expect to have two main components in the data: $W+2$ jets events and multijet events in which a jet has been misidentified as an electron (called QCD background in the following). $W+2$ jets events are simulated using the leading-order matrix-element program ALPGEN [11] for the Wjj process (i.e. production of $W+2$ partons, which are in our case gluons or u, d, s, c quarks, since the $Wb\bar{b}$ is simulated sepa-

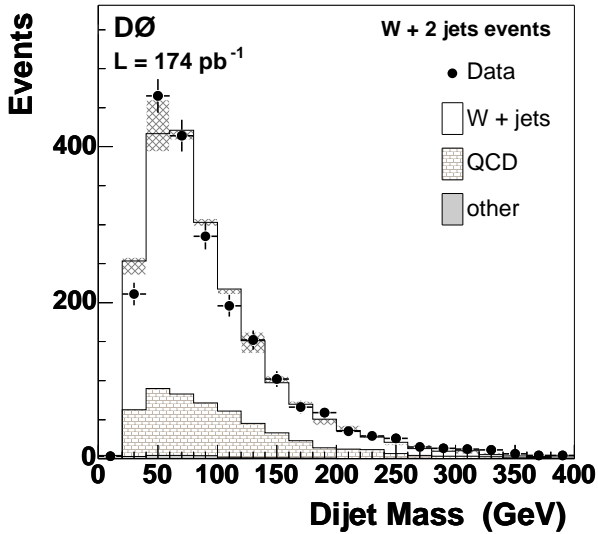


FIG. 1: Distribution of the dijet invariant mass of $W + 2$ jets events, compared with cumulative contributions from the QCD background (derived from data), the simulation of $W +$ jets events and the other SM backgrounds, which are small before b tagging. Uncertainties on the simulation from systematics of the jet energy scale are indicated by the hatched bands. The simulated contributions are normalized to the integrated luminosity of the data.

rately), followed by PYTHIA [12] for parton showering and hadronization. The QCD background is estimated from data using measured probabilities for jets to be misidentified and accepted as electrons.

The distribution of the dijet invariant mass in $W + 2$ jets events is shown in Fig. 1, where it is compared to expectation. The Wjj expectation is normalized to the data using the next-to-leading-order (NLO) MCFM calculation [13], providing a simulated rate for $W + 2$ jets events in agreement with the measured rate. Taking into account uncertainties originating from the jet energy scale, the shape of the distribution is also well described. The systematic uncertainty associated with the selection of exactly two jets in the final state has been studied in data and in simulations. The rates for $W + 3$ jets and $W + 4$ jets events, after normalizing to the $W + 2$ jets sample, are described by the ALPGEN and PYTHIA simulation to within 15% and 6%, respectively. The resulting systematic uncertainty on the expectation is $\pm 5\%$.

To search for $Wb\bar{b}$ final states and to suppress background, we apply the b -tagging algorithm to jets having at least two tracks, with $p_T^{track1(2)} > 1.0(0.5)$ GeV. These requirements have a typical efficiency per jet of 80% for multijets events, which is reproduced to within 5% by the simulation. The b -tagging algorithm uses a lifetime probability that is estimated from the tracks associated with a given jet. A small probability corresponds to jets having tracks with large impact parameters that charac-

terize b -hadron decays. Requiring a probability smaller than 0.7%, yields a mistag (tagging of u, d, s or gluon jets as b jets) rate of $(0.50 \pm 0.05)\%$. The tagging efficiency for a central b jet with p_T between 35 and 55 GeV is measured to be $(48 \pm 3)\%$.

The tagging efficiency in the simulation is adjusted to the one measured in data. A study of the p_T and η dependence in data and in simulation indicates a systematic uncertainty on tagging efficiencies of $\pm 6\%$. When tagging light quarks, there is a larger systematic uncertainty on the efficiency ($\pm 25\%$) that originates from the direct application of the algorithm to simulated events. This has only a small effect on the final results, since the fraction of events with two mistagged jets is $< 10\%$ of the total number of $W + 2$ b -tagged jets. For the tagging efficiency of c quarks, we use the same data/simulation efficiency ratio as for b quarks.

To reduce the presence of b jets from gluon splitting, and to help assure an unambiguous determination of jet flavors in simulation, we require the separation between the two reconstructed jets ($\Delta\mathcal{R}$) to be greater than 0.75. In Fig. 2 we show the distribution of the dijet mass for $W+2$ jets events in which at least one jet is b tagged. The data are well described by the sum of the multijet background and simulated SM processes (cf. Table I). The $t\bar{t}$ contribution is simulated with PYTHIA ($\sigma_{t\bar{t}} = 6.77 \pm 0.42$ pb [14]). Single-top production ($\sigma_{W^* \rightarrow tb} = 1.98 \pm 0.32$ pb, $\sigma_{gW \rightarrow tb} = 0.88 \pm 0.13$ pb [15]) is generated with COM-PHEP [16], assuming a top-quark mass of 175 GeV, and is shown in Fig. 2, in combination with other processes: $Z \rightarrow ee$, $W \rightarrow \tau\nu$ and $WZ(\rightarrow b\bar{b})$, which are simulated using PYTHIA with cross sections of 255 pb [17], 2775 pb [17], and 0.6 pb [13], respectively. As for the Wjj process, the $Wb\bar{b}$ contribution is simulated using ALPGEN and PYTHIA, requiring $p_T^b > 8$ GeV and $\Delta\mathcal{R}_{b\bar{b}} > 0.4$ at the parton level, with $\sigma_{Wb\bar{b}} = 3.35$ pb computed at NLO using the MCFM program. WH production is simulated with PYTHIA using the computed cross section at NLO, which depends on m_H [2].

To further improve signal/background, we select events in which a second jet is b tagged. The final results for the number of observed and expected events are given in Table I. Data from the last column are not used in the analysis, but provide a check of the accuracy of our expectations for events with two b -tagged jets in the control sample of $W + \geq 3$ jets events, which is dominated by $t\bar{t}$ production.

The distribution of the dijet mass for events with two b -tagged jets is shown in Fig. 3. The expected number of events is 4.4 ± 1.2 , of which 1.7 events are expected from $Wb\bar{b}$ production. The dominant systematic uncertainties on the expectation come from uncertainties on the b -tagging efficiency (11%) and jet energy corrections. The uncertainty on the latter propagates to uncertainties of 7% on $Wb\bar{b}$ production, 4% on single-top and WH production, and 3% on $t\bar{t}$ production. The total system-

atic uncertainty on the expectation is 26%, including the uncertainties on cross sections and luminosity (18% and 6.5%, respectively).

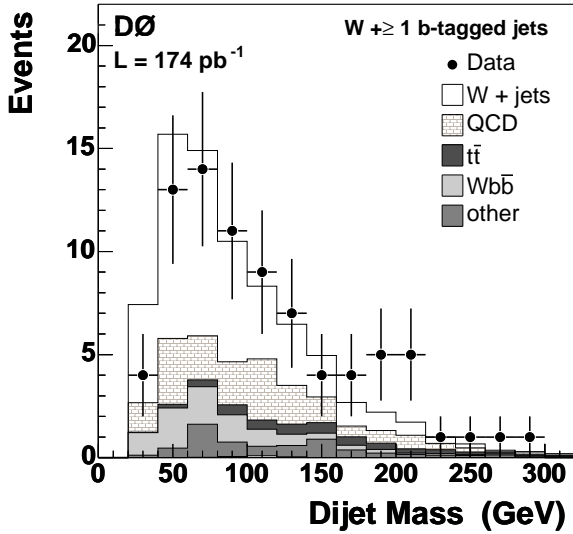


FIG. 2: Distribution of the dijet invariant mass for $W + 2$ jets events, when at least one jet is b tagged, compared to expectation (cumulative). The other SM backgrounds include single-top events. The simulated contributions are normalized to the integrated luminosity of the data.

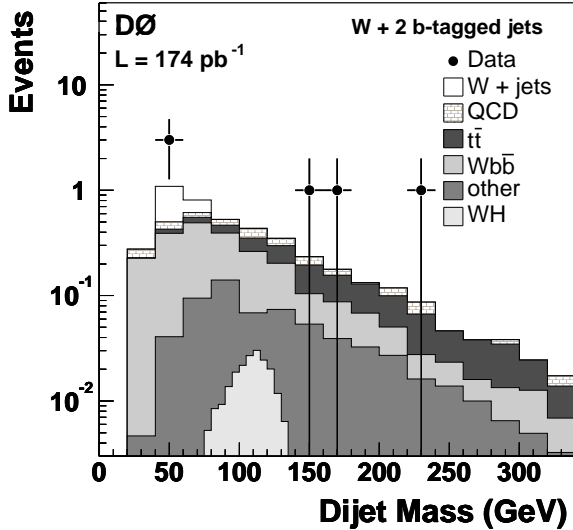


FIG. 3: Distribution of the dijet invariant mass for $W + 2$ b -tagged events, compared to expectation (cumulative). The simulated contributions are normalized to the integrated luminosity of the data. The expectation for a 115 GeV Higgs boson from WH production is also shown.

Assuming that the six observed events are consistent with the SM, without contributions from $Wb\bar{b}$ and WH , and using the $Wb\bar{b}$ signal efficiency of $(0.90 \pm 0.14)\%$, we set a 95% C.L. upper limit of 6.6 pb on the $Wb\bar{b}$ cross

section, for $p_T^b > 20$ GeV and $\Delta R_{bb} > 0.75$ [18]. The limits on the cross sections are obtained using a Bayesian approach [19] that takes account of both statistical and systematic uncertainties.

The expected contribution from the $b\bar{b}$ decay of a SM Higgs boson, with $m_H = 115$ GeV produced with a W , is also shown in Fig. 3, and amounts to 0.06 events. The mean and width of a Gaussian fit to this expected contribution in the mass window 85–135 GeV are 110 and 16 GeV, a relative resolution of $(14 \pm 1)\%$. Similar resolutions are obtained for Higgs-boson masses in the 105–135 GeV region.

No events are observed in the dijet mass window of 85–135 GeV. The expected SM background (including $Wb\bar{b}$) is 1.07 ± 0.26 events, and the expected WH signal is 0.049 ± 0.012 events, with a signal efficiency of $(0.21 \pm 0.03)\%$. In the absence of a signal, we set a limit on the cross section for $\sigma(p\bar{p} \rightarrow WH) \times BR(H \rightarrow b\bar{b})$ of 9.0 pb at the 95% C.L., for a 115 GeV Higgs boson.

The same study was performed for $m_H = 105, 125$ and 135 GeV, for which 0, 0 and 1 event were observed in the corresponding mass windows. The resulting limits (11.0, 9.1 and 12.2 pb, respectively) are compared to the SM expectation in Fig. 4, and to the results published by the CDF collaboration, using a smaller integrated luminosity of 109 pb^{-1} at $\sqrt{s} = 1.8$ TeV, but for combined e and μ channels [20].

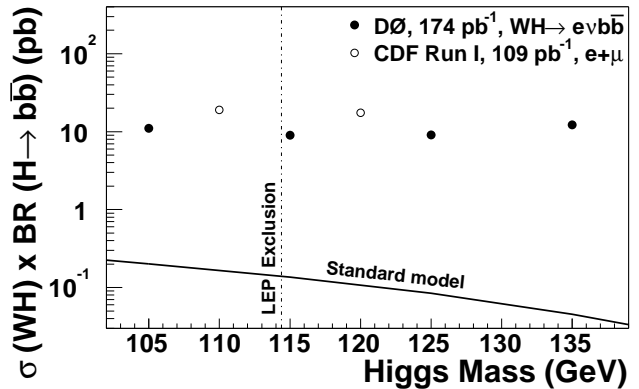


FIG. 4: 95% C.L. upper limit on $\sigma(p\bar{p} \rightarrow WH) \times BR(H \rightarrow b\bar{b})$ compared to the SM expectation at $\sqrt{s} = 1.96$ TeV, and to CDF results [20], which were obtained at $\sqrt{s} = 1.8$ TeV. The predicted WH cross section at 1.96 TeV is approximately 15% larger than that at 1.8 TeV.

In conclusion, we have performed a search for the $Wb\bar{b}$ final state, and have set an upper limit of 6.6 pb on this largest expected background to WH associated production. We have studied the dijet mass spectrum of two b -tagged jets in the region where we have the best sensitivity to a SM Higgs boson, and for Higgs-boson masses between 105 and 135 GeV we set 95% C.L. upper limits between 9.0 and 12.2 pb on the cross section for WH production multiplied by the branching ratio for $H \rightarrow b\bar{b}$.

TABLE I: Summary for the $e + \cancel{E}_T + \text{jets}$ final state: the numbers of expected $W + \geq 2$ jets and $W + 2$ jets events, before and after b tagging, originating from WH (for $m_H = 115$ GeV), WZ , $Wb\bar{b}$, top production ($t\bar{t}$ and single-top), QCD multijet background, and W or Z +jets (excluding $Wb\bar{b}$ which is counted separately) are compared to the numbers of observed events. The last column shows the same comparison for the control sample of $W + \geq 3$ jets events that contain two b -tagged jets.

	$W + \geq 2$ jets	$W + 2$ jets	$W + 2$ jets (1 b -tagged jet)	$W + 2$ jets (2 b -tagged jets)	$W + \geq 3$ jets (2 b -tagged jets)
WH	0.6 ± 0.1	0.4 ± 0.1	0.14 ± 0.03	0.056 ± 0.013	0.015 ± 0.004
WZ	1.4 ± 0.3	1.2 ± 0.3	0.38 ± 0.09	0.13 ± 0.03	0.02 ± 0.01
$Wb\bar{b}$	24.7 ± 6.2	21.4 ± 5.3	6.6 ± 1.5	1.72 ± 0.41	0.37 ± 0.09
$t\bar{t}$	41.4 ± 8.7	8.6 ± 1.8	2.7 ± 0.6	0.78 ± 0.19	4.63 ± 1.11
Single-top	11.6 ± 2.4	8.3 ± 1.7	2.7 ± 0.6	0.47 ± 0.11	0.30 ± 0.07
QCD multijet	492 ± 108	393 ± 86	17.1 ± 4.3	0.50 ± 0.20	0.92 ± 0.37
W or Z +jets	2008 ± 502	1672 ± 418	43.0 ± 12.9	0.78 ± 0.22	0.86 ± 0.24
Total expectation	2580 ± 626	2106 ± 513	72.6 ± 20.0	4.44 ± 1.17	7.12 ± 1.89
Observed events	2540	2116	76	6	7

We thank the staffs at Fermilab and collaborating institutions, and acknowledge support from the Department of Energy and National Science Foundation (USA), Commissariat à l’Energie Atomique and CNRS/Institut National de Physique Nucléaire et de Physique des Particules (France), Ministry of Education and Science, Agency for Atomic Energy and RF President Grants Program (Russia), CAPES, CNPq, FAPERJ, FAPESP and FUNDUNESP (Brazil), Departments of Atomic Energy and Science and Technology (India), Colciencias (Colombia), CONACyT (Mexico), KRF (Korea), CONICET and UBACyT (Argentina), The Foundation for Fundamental Research on Matter (The Netherlands), PPARC (United Kingdom), Ministry of Education (Czech Republic), Natural Sciences and Engineering Research Council and WestGrid Project (Canada), BMBF and DFG (Germany), A.P. Sloan Foundation, Research Corporation, Texas Advanced Research Program, and the Alexander von Humboldt Foundation.

submission to Nucl. Instrum. Methods Phys. Res. A, and T. LeCompte and H.T. Diehl, Ann. Rev. Nucl. Part. Sci. **50**, 71 (2000).

- [4] The pseudorapidity is defined as a function of the polar angle θ as $\eta \equiv -\ln(\tan \frac{\theta}{2})$.
- [5] S. Abachi *et al.* (DØ Collaboration), Nucl. Instrum. Methods Phys. Res. A **338**, 185 (1994).
- [6] S. Beauceron, Ph. D. Thesis, University of Paris VI, 2004 (unpublished).
- [7] The muon is considered isolated if its distance from the closest jet is $\Delta\mathcal{R} > 0.4$.
- [8] G. Blazey *et al.*, in *Proceedings of the workshop “QCD and Weak Boson Physics in Run II”*, edited by U. Baur, R.K. Ellis, and D. Zeppenfeld, Batavia (2000) p. 47.
- [9] S. Greder, Ph. D. Thesis, University Louis Pasteur, Strasbourg, 2004 (unpublished).
- [10] R. Brun and F. Carminati, CERN Program Library Long Writeup W5013 (1993).
- [11] M. Mangano *et al.*, hep-ph/0206293 (2002), JHEP 0307, 1 (2003).
- [12] T. Sjöstrand *et al.*, Comput. Phys. Commun. **135**, 238 (2001).
- [13] J. Campbell and K. Ellis, <http://mcfm.fnal.gov/> and Phys. Rev. D **65**, 113007 (2002).
- [14] N. Kidonakis and R. Vogt, Phys. Rev. D **68**, 114014 (2003).
- [15] E. Laenen, hep-ph/0308025 (2003).
- [16] A. Pukhov *et al.*, hep-ph/9908288 (1999).
- [17] D. Acosta *et al.* (CDF Collaboration), hep-ex/0406078, subm. to Phys. Rev. Lett. For $\sigma(W \rightarrow \tau\nu)$ we use $\sigma(W \rightarrow \ell\nu)$ from this Ref. assuming lepton universality.
- [18] The NLO MCFM calculation gives $\sigma_{Wb\bar{b}} = 0.75$ pb for parton level cuts $p_T^b > 20$ GeV and $\Delta\mathcal{R}_{b\bar{b}} > 0.75$.
- [19] I. Bertram *et al.*, Fermilab-TM-2104 (2000).
- [20] F. Abe *et al.* (CDF Collaboration), Phys. Rev. Lett. **82**, 2038 (1999).

[*] Visitor from University of Zurich, Zurich, Switzerland.

[†] Visitor from Institute of Nuclear Physics, Krakow, Poland.

- [1] S. Eidelman *et al.*, Phys. Lett. B **592**, 1 (2004); LEP electroweak working group, <http://lepewwwg.web.cern.ch/LEPEWWG/>
- [2] T. Han and S. Willenbrock, Phys. Lett. B **273**, 167 (1991); S. Mrenna and C.P. Yuan, Phys. Lett. B **416** 200 (1998); M. Spira, Fortsch. Phys **46** 203 (1998).
- [3] V. Abazov *et al.* (DØ Collaboration), in preparation for